31st Annual International Conference of the IEEE EMBS
Minneapolis, Minnesota, USA, September 2-6, 2009

Spike Library Based Simulator for Extracellular Single Unit Neuronal Signals

P. T. Thorbergsson, *Student Member, IEEE*, H. Jorntell, F. Bengtsson, M. Garwicz, J. Schouenborg, A. J Johansson, *Member, IEEE*

***Abstract*— A well defined set of design criteria is of great importance in the process of designing brain machine interfaces (BMI) based on extracellular recordings with chronically implanted micro-electrode arrays in the central nervous system (CNS). In order to compare algorithms and evaluate their performance under various circumstances, ground truth about their input needs to be present. Obtaining ground truth from real data would require optimal algorithms to be used, given that those exist. This is not possible since it relies on the very algorithms that are to be evaluated. Using realistic models of the recording situation facilitates the simulation of extracellular recordings. The simulation gives access to a priori known signal characteristics such as spike times and identities. In this paper, we describe a simulator based on a library of spikes obtained from recordings in the cat cerebellum and observed statistics of neuronal behavior during spontaneous activity. The simulator has proved to be useful in the task of generating extracellular recordings with realistic background noise and known ground truth to use in the evaluation of algorithms for spike detection and sorting.**

I. INTRODUCTION

One of the current promising trends in the field of brain-machine interfaces (BMI) is development toward long term extracellular recordings with chronically implanted multi-electrode arrays (MEA) in the central nervous system (CNS). Detection and classification of spikes are of major importance to successful implementation of a BMI based on extracellular recordings.

The algorithms chosen for spike detection and classification will determine the design criteria for signal acquisition hardware. However, the task of choosing an algorithm is not a trivial one making qualitative evaluation of their performance necessary.

In order to evaluate the performance of algorithms for spike detection and classification under various hardware implementations, we have chosen to implement a simulator to generate extracellular recordings. Simulation gives access to ground truth about spiking activity in the recording and thereby facilitates a quantitative assessment of algorithm performance since the characteristics of the signals are known a priori.

This work was supported by a Linnaeus Grant from the Swedish Research Council, ID: 60012701 and a grant from the Knut and Alice Wallenberg Foundation, nr 2004.0119.

P. T. Thorbergsson and A. J Johansson are with the Neuronano Research Center and at Dept. of Electrical and Information Technology, both at Lund University, Lund, Sweden. H. Jorntell, F. Bengtsson, M. Garwicz and J. Schouenborg are with the Neuronano Research Center and at the Dept. of Experimental Medical Science, both at Lund University, Lund, Sweden.

E-mail: palmi.thor.thorbergsson@eit.lth.se

Similar approaches have been taken by others to perform the task of algorithm assessment. However, not many simulators have been fully published, making it necessary for researchers to implement their own versions. Previous works include [1], [2] and [3], where simulators based on the same ideas as ours were used. A fully documented simulator based on analytical models has been published in [4]. In contrast, we have developed a simulator based on large amounts of extracellular recordings that is more readily applicable to our experimental setups.

The simulator described in this paper is fully documented and will be published for general use under a *Creative Commons* license [5] as a library of *MATLAB®* functions along with an extensive and expandable spike library. The performance of the simulator has been successfully verified by comparing features such as firing statistics, power spectral density and autocorrelation of simulated and real signals.

II. MODELS

A. Neuronal Distribution and Density

Neuronal density varies among structures in the CNS. We have chosen to use a modified density estimate provided by [6]. In this work, the number of hippocampal CA1 pyramidal cells contained within a cylinder of a given radius was estimated.

Our modification involves replacing the cylinder with a sphere of equal radius but assuming the same number of neurons. The motivation behind this modification is that we want to simulate activity in CNS structures that do not necessarily have the prominent laminar organization that is encountered in the hippocampus [7]. We further assume an isotropic neuronal distribution. Figure 1 shows how the recording environment is modeled.

B. Unit Isolation

In the default setup of the simulator we assume the volume surrounding the electrode to be divided into two parts; “near field” and “far field”. The surfaces of the inner and outer spheres shown in Figure 1 bound the two volumes. Spikes coming from neurons within the near field and the far field are referred to as target units and noise units respectively. We assume a small amount of active target units to be present in the near field and we assume those to be separable from the noisy background activity contributed by the noise units in the far field.

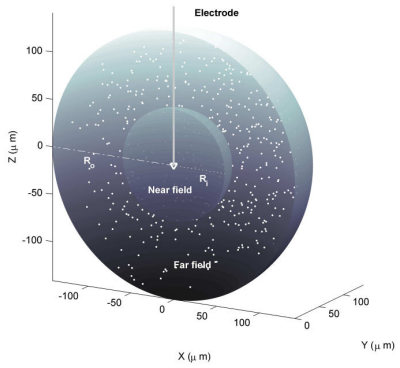

Fig. 1. A model of the recording environment. The white dots in the far field represent noise units. Target units are placed in the near field.

C. Extracellular Spike Amplitude

The variation in spike shape and amplitude has been studied by [6], [8] and [9]. Our amplitude model for the noise units is based on the result in [9] that at large distances (in the electrode's far field), the amplitude decays as $1/r^n$ where n is between 2 and 3. We have not included the spatially dependent lowpass filtering also described in [9] since the spike prototypes in our library are obtained from actual recordings and are therefore assumed to have undergone this filtering already.

Based on observations of simulated and real signals in combination with the work mentioned above, we model the normalized spike amplitude decay as

$$A = \begin{cases} \frac{1}{(Kr+1)^2} & \text{for noise units} \\ 1 & \text{for target units} \end{cases} \quad (1)$$

where K is a scaling factor that specifies the rate of decay. Within the near field of the electrode we currently assume a constant amplitude of one.

D. Inter Spike Interval and Refractory Period

To generate spike times for our target and noise units, we assume a renewal process with gamma distributed inter spike intervals (ISI). An advantage of this assumption is that both the absolute and relative refractory periods are directly implemented in the model [10]. The spike times $\tau_p(n)$ for unit p are thus given by

$$\tau_p(n) = \sum_{j=1}^{n} ISI_j \quad , \quad ISI \sim \Gamma(k, \theta) \quad (2)$$

where k and θ are the shape and scale factors of the gamma distribution respectively. The value of the shape factor varies among units with different mean firing rates $\overline{f}$, but an appropriate value can be obtained by estimating parameters in a real ISI distribution (see Figure 4). By definition of the gamma distribution, the scale factor is determined by the mean ISI, $\overline{ISI}$, and shape factor k

$$\theta = \frac{\overline{ISI}}{k} = \frac{1}{\overline{f}k}. \quad (3)$$

E. Noise

We assume that the background noise mainly consists of the sum of scaled spike trains generated by noise neurons in the far field of the electrode. The scaling factor is the same as the amplitude decay in Equation 1. Apart from the amplitude decay, the noise contributing spike trains are generated in the same way as the target unit spike trains. Instead of assuming a common mean firing rate for all noise units, the firing rate for each noise unit is drawn from a uniform distribution bounded by values given by the user.

We assume thermal noise to be present at the input of the recording amplifier. The root-mean-square (RMS) of the thermal noise can be expressed as

$$\sqrt{\bar{e}_n^2} = \sqrt{4kTRB} \quad (4)$$

where k is Boltzmann's constant, T is the temperature, R is the input resistance of the recording system (electrode and amplifier) and B is the system's bandwidth [11]. The values of those parameters can be adjusted to match an actual setup, but typical values for an implanted system ($T = 310K$, $R = 1M\Omega$, $B = 10kHz$) will give RMS values around $13\mu V$ at the amplifier input.

F. Model limitations

The models have limitations in the assumptions of the dynamics and stationarity of the underlying processes. Correlation between different spike trains and bursting activity is not accounted for and we assume constant spike morphologies throughout the duration of the simulation. Further, non-spiking activity (passive signaling [7]) is not accounted for and the assumptions of isotropic neuronal distribution and absence of amplitude decay in the electrode's near field are simplifications worth bearing in mind.

III. SPIKE LIBRARY

Spike waveforms were detected in and extracted from recordings performed in various regions in the cat cerebellum [12] and sorted using the open-source software package *Chronux* [13][14]. Thresholds for spike detection were set automatically using the method described in [1]. The average waveforms were upsampled to 100ksps and stored. Executing this process on an ensemble of recordings containing well isolated single unit activity resulted in a library consisting of 85 different waveforms.

To obtain a qualitative measure of the characteristics of the spike library, we looked at features such as spike duration, frequency contents and general morphology of the stored spikes. The results of the frequency analysis are not shown here since they correlate strongly with spike duration. This examination showed us that the library is sufficient as a basis for modeling the recordings needed for our future algorithm assessment.

We define spike duration as the time period where the absolute amplitude of the largest phase of the spike is above half its peak value. The spike duration histogram in Figure 2 shows that the vast majority of spikes have durations that

classifies them as fast spikes [8]. This provides us with an upper bound for testing the algorithms since fast spikes are assumed to pose the biggest challenge to them and is therefore regarded as a desirable feature. Figure 2 also shows five representative spikes from the library.

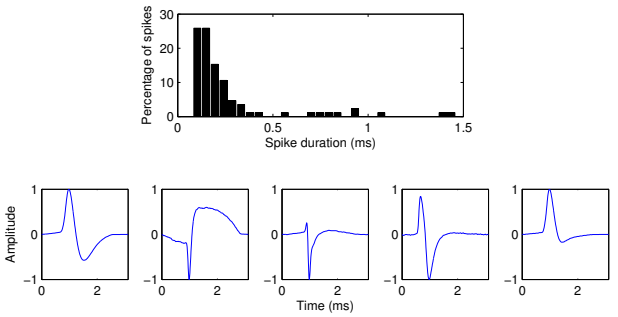

Fig. 2. Spike duration histogram (upper) and five spike from the spike library that demonstrate various spike morphologies present in the library (lower).

IV. ALGORITHM

The basic ideas behind the simulation algorithm are inspired by the simulator described in [1]. The algorithm is summarized in Algorithm 1.

The user provides the algorithm with input such as duration of the recording (D), sampling rate (f_s), number of target neurons (N_u), standard deviation of physiological background noise (σ_n), parameters of thermal noise (T, R, B), mean firing rate of target units (f_u), a range of firing rates for noise units (f_n) and rate of amplitude decay in far field (K). For each noise neuron, a firing rate is drawn from a uniform distribution bounded by the given values. In the case of multiple target units, the mean firing rates of the individual units can be set separately.

For each of the target units, spike times are generated (Equation 2) and a random spike waveform is chosen from the spike library. The waveform is then added to the recording with unchanged amplitude at the obtained spike times.

To generate the background noise, each noise unit is assigned a random position in the far field of the recording electrode (see Figure 1) and a random firing rate is chosen. The amplitude of the unit is then derived from it's distance from the electrode tip (Equation 1). The noise units' spike times are generated in the same way as the target units' and they are added to the recording trace in the same manner as well. White noise is generated according to Equation 4 and added to the recording.

The output of the simulation is the spike times and labels of all (target) spikes in the recording, the simulated recording and background noise as well as the actual waveforms of the target units as taken from the spike library.

Input: Duration of recording, sampling rate, number of target units, standard deviation of physiological noise, thermal noise parameters, mean firing rates, rate of amplitude decay in far field.

Output: Target unit spike times, entire recording, noise component of recording, target unit waveforms.

foreach *Noise/target unit* P **do**

Generate a spike train $s_p(t)$ of N spikes w_k with amplitude A_p (Equation 1) occurring at $\tau_p(n)$ (Equation 2):

$$s_p(t) = A_p \sum_{n=1}^{N} w_k(t - \tau_p(n)) \quad , \quad k \sim U(1, L)$$

where k is the index of the selected spike waveform and L is the number of spikes in the library.

end

Add the spike trains and thermal noise $e(t)$ to obtain the final signal $v(t)$:

$$v(t) = \sum_{p=1}^{P} s_p(t) + e(t)$$

Algorithm 1: The extracellular recording simulator.

V. VERIFICATION OF PERFORMANCE

A. Methods

To evaluate the performance of the simulator, we selected a set of segments from our recordings and roughly estimated features such as number of separable units, mean firing rates and level of background noise. In order to try to mimic the real recordings, these estimates were used as input parameters to the simulator. Since the modeling of the background noise has proved to be the most challenging task in the implementation, we focused our attention toward segments with low target unit activity and low signal-to-noise ratio (SNR). We then compared the autocorrleation [3] and its Fourier transform, the power spectral density (PSD), for real and simulated signals to get a qualitative assessment of the similarities. The PSD was estimated with Welch's method. Results from both analyses (averages over four segments of data) are shown in Figure 3 to facilitate comparison with results from earlier studies. To evaluate the validity of the assumption of gamma distributed inter spike intervals, we fitted a gamma distribution to inter spike intervals obtained from in-vivo recordings.

To demonstrate the usefulness of the simulator in the task of calculating the probability of detection and false positives in spike detection, we ran a batch of simulated signals through a spike detection algorithm and calculated the resulting probabilities.

B. Results

The comparison between the power spectral densities of the real and simulated signals revealed strong similarities (see Figure 3(a)). The densities resemble those obtained by [8] when studying frequency contents of background activity in extracellular recordings.

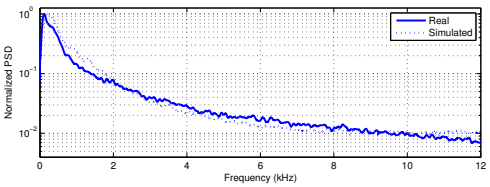

(a) Power spectral density of real and simulated recordings. The simulation parameters were $N_u = 5$, $f_u = 10$, $f_n \sim U(1, 50)$, $\sigma_n = 0.2$, $K = 0.05$.

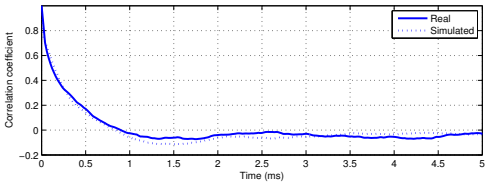

(b) Autocorrelation of real and simulated recordings.

Fig. 3. A comparison of real and simulated recordings

The properties of the PSD are influenced by the modeling of the background noise. Assuming varying activity among neurons and assigning random mean firing rates to the noise neurons gave a good match.

The autocorrelation of the simulated and real signals (Figure 3(b)) showed strong similarities. Reference [3] reported significant autocorrelation at delays up to around 1.2 ms. The shorter interval in our results is mainly caused by the fact that our spike library is dominated by fast spikes. We ran simulations with synthetic spikes of various durations as well and saw a clear connection between the duration of significant autocorrelation and "dominating" spike duration in the library.

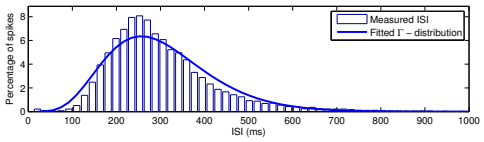

Fig. 4. Measured ISI during spontaneous activity of a single neuron. The parameters of the fitted gamma distribution are $k = 6.4$ and $\theta = 0.047$.

Figure 4 shows a histogram of measured ISI during typical spontaneous activity of a single neuron in the cat cerebellum. The histogram and the fitted gamma distribution show close resemblance and support the assumption of gamma distributed ISI [10].

Figure 5 shows a short segment of a simulated signal and demonstrates the usability when testing spike detection with a threshold crossing criterion. In this case, the probability of detection and false positives was $P_D = 95.35\%$ and $P_{FP} = 4.13\%$ respectively.

VI. CONCLUSIONS AND FUTURE WORK

A simulator based on extracellular spikes and observed statistics of neuronal firing has been implemented and tested. The simulator has proved to be useful for providing simulated extracellular recordings to use in the evaluation of algorithms for spike detection and sorting.

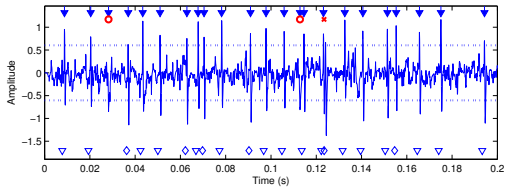

Fig. 5. A short segment of a simulated recording. The diamonds (◇) and triangles (▽) at the bottom indicate the beginning of spikes belonging to two target units present in the recording (ground truth). The arrows at the top indicate detected spike times obtained with a double amplitude threshold (dotted lines). The circles and crosses at the top indicate false positives and missed spikes respectively.

The simulator will be fully published along with an expandable spike library. In [14], some problems behind diverse conventions in methodology are mentioned. We believe that a joint effort would make the resulting research more straight forward and applicable. Our aim is to establish an open venue for researchers to submit their spike libraries and additions to the algorithm. Increased size of the library and more detailed information on specific regions in the CNS will facilitate the simulation of activity in specific areas of the CNS.

Reducing the limitations of the simulator is a work in progress. We plan to investigate appropriate and biologically valid ways of modeling the correlation between target units and implement time-varying firing statistics. These features will be added to the simulator as they come along.

REFERENCES

[1] R. Quiroga, Z. Nadasdy, and Y. Ben-Shaul. Unsupervised spike detection and sorting with wavelets and superparamagnetic clustering, *Neural Comp.*, vol. 16, no. 8, pp. 1661-1687, Aug. 2004.

[2] S. Gibson, J.W. Judy, D. Markovic. Comparison of spike-sorting algorithms for future hardware implementation. *Conference proceedings: Annual International Conference of the IEEE Engineering in Medicine and Biology Society*, vol. 1, pp. 5015-20, 2008.

[3] U. Rutishauser et al. Online detection and sorting of extracellularly recorded action potentials in human medial temporal lobe recordings, in vivo, *Journal of Neuroscience Methods*, vol. 154, pp. 204-224, 30 Jun. 2006.

[4] L.S. Smith, N. Mtetwa. A tool for synthesizing spike trains with realistic interference, *Journal of Neuroscience Methods*, vol. 159, pp. 170-180, Jan. 2007.

[5] Website: *Creative Commons*, http://creativecommons.org.

[6] D.A. Henze et al. Intracellular Features Predicted by Extracellular Recordings in the Hippocampus In Vivo, *Journal of Neurophysiology*, vol. 84, pp. 390-400, 2000.

[7] E.R. Kandel et al. *Principles of Neural Science, Fourth Edition*, McGraw-Hill, USA, 2000.

[8] M.S. Fee, P. Mitra, and D. Kleinfeld. Variability of Extracellular Spike Waveforms of Cortical Neurons, *Journal of Neurophysiology*, vol. 76, pp. 3823-3833, Dec. 1996.

[9] K.H. Pettersen, and G.T. Einevoll. Amplitude Variability and Extracellular Low-Pass Filtering of Neuronal Spikes, *Biophysical Journal*, vol. 94, pp. 784-802, 2008.

[10] D. Heeger. Poisson Model of Spike Generation, technical report, 2000, http://www.cns.nyu.edu/∼david/ftp/handouts/poisson.pdf.

[11] R. Pettai. *Noise In Receiving Systems*, John Wiley & Sons, USA, 1984.

[12] *Jörntell, H.* & Ekerot, C.F. Reciprocal bidirectional plasticity of parallel fiber receptive fields in cerebellar Purkinje cells and their afferent interneurons. /Neuron/ *34*, 797-806 (2002).

[13] Website: *Chronux Analysis Software*, http://www.chronux.org.

[14] P. Mitra, H. Bokil. *Observed Brain Dynamics*, Oxford University Press, USA, 2008.